Interpretation of FAENA and TIFFSS experiments : Comparison of fatigue strength evaluation methods on thermal striping

(Research Report)

Septembr 2000

Japan Nuclear Cycle Development Institute
O-arai Engineering Center

〒319-1184　茨城県那珂郡東海村村松4番地49
核燃料サイクル開発機構
技術展開部　技術協力課

Ⓢ

Interpretation of FAENA and TIFFSS experiments : Comparison of fatigue strength evaluation methods on thermal striping

(Research Report)

Naoto KASAHARA* and Yves LEJEAIL**

Abstract

Since thermal striping is a coupled thermohydraulic and thermomechanical phenomenon, sodium mock-up tests were usually required to confirm structural integrity. CEA and JNC have developed evaluation procedures of thermal striping to establish design-by-analysis methodology for this phenomenon. In order to compare and to validate these methods, two benchmark problems were planned under EJCC contract. One of benchmarks provided by CEA is temperature and fatigue evaluation of tubes and plates tests performed with the FAENA facility. Another problem from JNC is the same evaluation of plates tests conducted by the TIFFSS facility. This report describes the results of intercomparison of fatigue strength evaluation methods through application to both FAENA and TIFFFSS experiments.

* Structure and Material Research Group, System Engineering Division, OEC, JNC
** CEA-Cadarache DER/SERSI/LECC

FAENAおよびTIFFSS試験評価：
サーマルストライピング疲労評価法および評価結果の比較

（研究報告書）

笠原 直人*、Yves LEJEAIL**

要　旨

流体温度ゆらぎによる構造物の熱疲労現象は熱流動と構造の両分野に亘る複雑な問題であり、従来その評価にはナトリウムモックアップテストが必要であった。本問題に対する解析による設計法を確立するため、CEAとJNCは評価法の開発を行ってきている。流体温度ゆらぎに対する構造健全性に対して、流体から構造への伝達過程で生じる温度ゆらぎの減衰作用が重要な役割を果たすことが知られている。その減衰の大きさは周波数に依存することから、評価法検証のために周波数制御ナトリウム試験データを用いたベンチマーク問題を計画した。一つはCEAから出題されたもので、温度が周波数制御された平行流を受ける管と平板の温度および疲労評価に関する問題である。もう一つのJNC出題の問題は、周波数制御された垂直ジェットを受ける平板の評価に関するものである。本報告書は両者の実験の疲労評価結果について述べる。応力計算にCEAは有限要素解析法を、JNCは周波数応答関数を用いており、解析結果はCEAの算出応力がJNCより若干大きめであった。その結果、予測疲労損傷もCEAの結果が若干JNCより大きくなった。応力に差が生じた理由は、実験による温度波形が周波数応答関数で想定した正弦波と矩形波の中位にあることである。

尚、本内容は1999年9月から2000年8月までの期間にCEAカダラッシュ研究所にて実施した業務の一部である。

*)　大洗工学センター システム技術開発部 構造材料技術開発グループ
**)　CEAカダラッシュ研究所 炉心機器研究室

Contents

List of tables

List of figures

NOMENCLATURE

$T_f(t)$: Temperature of fluid

ΔT_f : Amplitude of sinusoidal temperature fluctuation of fluid

T_{fm}: Average temperature of fluid

$T_s(x,t)$: Temperature of structure

ΔT_s : Amplitude of sinusoidal temperature fluctuation on the structural surface

$T_{s\,max}$: Maximum temperature on the structural surface

$\sigma(x,t)$: Stress in structure

$\Delta\sigma|_{x=0}$: Amplitude of sinusoidal stress fluctuation on the structural surface

$\Delta\sigma_i$: Ideal stress range converted from hundred percent of fluid temperature amplitude

$G(x,t)$: Time response function of structure to fluid temperature fluctuation

$H(t)$: Time response function of effective heat transfer

$S(x,t)$: Time response function of effective thermal stress

$\phi\{T_s(x,t)\}$: Thermal stress function determined by mechanical boundary conditions

$T_f(s)$: Laplace transform of $T_f(t)$

$T_s(x,s)$: Laplace transform of $T_s(x,t)$

$G(x,s)$: Laplace transform of $G(x,t)$

$H(s)$: Laplace transform of $H(t)$

$S(x,s)$: Laplace transform of $S(x,t)$

$\Phi\{T_s(x,s)\}$: Laplace transform of $\phi\{T_s(x,t)\}$

$G(B_i, jf^*)$: Frequency response function of structural surface to fluid temperature fluctuation

$H(B_i, jf^*)$: Frequency response function of effective heat transfer

$S(jf^*)$: Frequency response function of effective thermal stress on the surface

$Bi = \dfrac{hL}{\lambda}$: Biot number

$t^* = \dfrac{ta}{L^2}$: Fourier number

$f^* = \dfrac{fL^2}{a}$: Non-dimensional frequency

x: Length from the surface of structure

t: Time

f: Frequency of sinusoidal fluctuation

h: Heat transfer coefficient

L: Wall thickness of structure

A: Area

V: Volume

a: Thermal diffusivity of structural material

λ : Heat conductivity of structural material

c: Specific heat

ρ : Density

E : $Young's$ modulus of structural material

α : Linear expansion coefficient of structural material

ν : $Poisson's$ ratio of structural material

σ_y : Yield stress of a material

K: Stress index determined by mechanical boundary conditions and material properties

$K = 1/(1-\nu)$ in the case of biaxial plane stress condition

D_f : Fatigue damage factor

N: Cycle number

N_f : Allowable cycle number of structural material

$\Delta \varepsilon_{tot}$: Strain range

1 INTRODUCTION

At incomplete mixing areas of high and low temperature fluids near the structural surface, temperature fluctuation of fluid gives thermal fatigue damage on the wall structures. This coupled thermohydraulic and thermomechanical phenomenon is called thermal striping, which has so complex mechanism and sometimes causes crack initiation on the structural surfaces that sodium mock-up tests are usually required to confirm structural integrity of components.

In order to establish design-by-analysis methodology for thermal striping, CEA and JNC have developed evaluation procedures of this phenomenon. Under EJCC framework, intercomparison of both procedures was planned through application to the common benchmark problems.

One of benchmarks provided by Dr. Yves LEJEAIL is temperature and fatigue evaluation of tubes and plates due to channel flows [1]. Another problem from JNC is the same evaluation of plates subjected to a vertical jet. The former test was performed by the FAENA facility at CEA-Cadarache. The later one was conducted with the TIFFSS facility at Hitachi Company.

Thermal striping evaluation procedures are divided into temperature analysis methods and fatigue evaluation methods.

The objective of this report is comparison and validation of fatigue strength evaluation methods with application to FAENA and TIFFSS sodium experiments.

Thermal stress caused by temperature fluctuation was sensitive to temperature distribution in structures and constraint conditions. In FAENA facility, inner surfaces of specimens were due to fluid temperature fluctuations and outer surfaces were surrounded by gas environment. FAENA-3 specimens are cylinders that have bending constraint characteristics. On the other hand, both sides of specimen were dipped in sodium in TIFFSS facility. TIFFSS-4 specimens are plates with different boundary conditions. One is a simple plate that has peak stress constraint characteristics and the other is a partially insulated plate which constraints bending plus membrane stresses.

It is required in this benchmark problem to take above characteristics of FAENA and TIFFSS experiments.

2. CEA EVALUATION

The following part deals with fatigue analysis of FAENA 3rd test by finite element method. First we have to briefly recall the principle of interpretations, since it combines experimental and computational methods.

2.1. PRINCIPLE OF INTERPRETATIONS OF FAENA TESTS

As explained in a precedent report, the tubular specimens are submitted to alternative injections of hot and cold sodium jets, at high frequency (0.07Hz and 0.3 Hz for FAENA 3rd serie. A schema of principle is given on Fig 2.1). Thus, crack pattern is initiated after a given number of cycles depending of temperature variation (due to the thickness of the tube (22.05 mm), temperature field has high radial gradients and induces thermal stresses inside the tube). A gradient of cracking is also created along axial direction, owing to a decrease of thermal loads in the same direction. The explanation is rather simple :

- consider the beginning of a cold sodium injection phase : the tube is hot at this instant due to the precedent shock. During the flowing of cold sodium (corresponding to increase of sodium position on z axis), the temperature of the liquid metal increases since it exchanges heat with the surface of the specimen
- the same process exists during hot sodium injection period : hot sodium temperature decreases during hot sodium flow by heat loss induced by the contact with the cold specimen

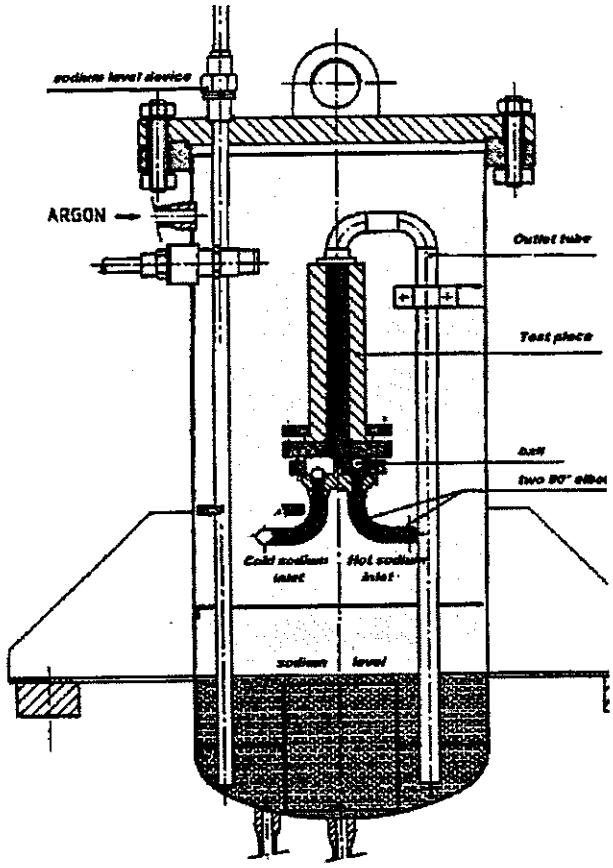

Fig.2.1 schema of injection system in FAENA sodium loop

This leads to a gradient of temperature variation along z axis, and then to a decrease of mechanical strain variation.

The interpretation requires the determination of the level z of the last observed crack corresponding to the initiation criteria, as reported on figure 2.2. Then we need to calculate the temperature, stress and strain profile in the section corresponding to the level of crack initiation in order to plot the point ($\Delta \varepsilon$, Ni) (i.e. strain variation , number of applied cycles).

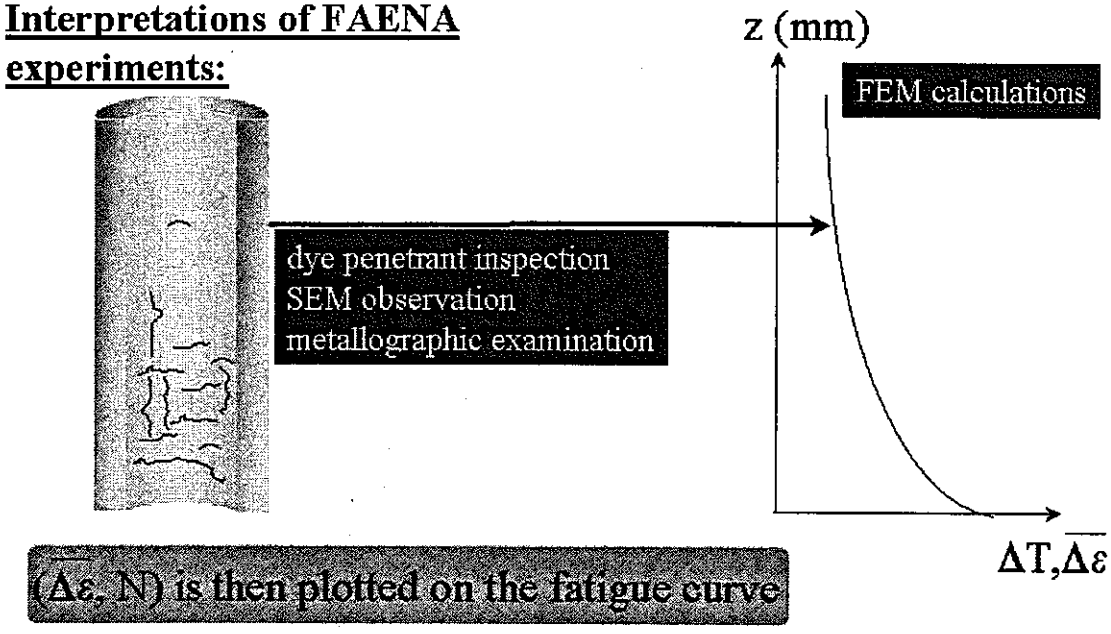

Fig.2.2 : principle of interpretation of FAENA experiments

The table 2.1 gives the level of crack initiation (or of maximum thermal load if there is no crack initiation) for the FAENA 3rd series

Table 2.1 : location of last crack observed

flow rate (l/h)	frequency (Hz)	inlet temperature variation in sodium (peak to peak) (°C)	outlet temperature variation in sodium (peak to peak) (°C)	z (mm)	ΔT(z) variation in sodium (°C)	time acquisition (s)
712	0.3	200	100	60	158	10
727	0.07	289	202	43 (no crack)	268	32

2.2. CALCULATION BY FINITE ELEMENT METHOD

2.2.1. THERMAL EVALUATIONS

The mesh of figure 2.3 was used in axisymetric mode, with 15 elements in the thickness.

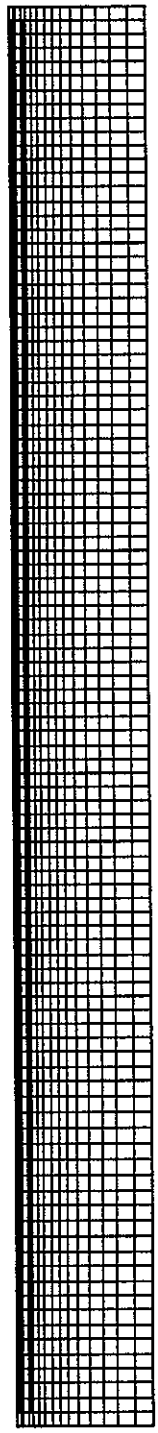

Fig.2.3 : mesh used for the simulations

The thermal calculation was an adjustment on the experimental temperature measurements. The following thermal characteristics, mean values for 316L at 370°C, were used for the tubes in our calculations :

Table 2.2 : location of last crack observed

thermal conductivity	specific heat	density
λ (W/mm/°C)	C (J/kg/°C)	ρ (kg/mm^3)
$19.2\ 10^{-3}$	581.9	$7.71\ 10^{-6}$

For the precise definition of fluid thermal loadings, basic functions have been determined :

$\Delta T_f(z) = (z + 152592.6) / (z + 527)$ (z in mm , frequency 0.07Hz) (2.1)

$\Delta T_f(z) = (z + 45398.7) / (z + 227.4)$ (z in mm , frequency 0.3Hz) (2.2)

Time history functions have been defined for each frequency. For f = 0.07Hz :

Table 2.3 : time function for the fluid temperature determination (0.07Hz)

t (s)	0	1.29	2.245	3.946	6.806	7.918	8.98	10.748	14.42	15.23
F(t)	0	0.669	0.786	0.903	1.	0.	-0.619	-0.826	-1.	-0.

For f = 0.3Hz :

Table 2.4 : time function for the fluid temperature determination (0.3Hz)

t (s)	0	0.63	1.41	1.61	2.21	2.70	3.31	3.56	4.
F(t)	0	0.5	1.	1.	0..	-0.4375	-1.	-1.	0.

Finally, in sodium temperature were evaluated by T_f (z,t) = $\Delta T_f(z)$ F(t) ; this temperature was simulated by heat flux equal to 0.727 Tf (z,t) / 289.5 imposed at the internal surface for frequency 0.07 Hz (respectively 0.727 T_f (z,t) / 190 for the frequency 0.3Hz). The numbers 289.5 and 190 are useful to normalize the temperature variation (which becomes equal to unity for the inlet z = 0). The imposed flux was necessary to adjust experimental measurement inside the thickness of the tubes as shown on figures 2.4 and 2.5 (the coefficient 0.727 was found to give the better agreement for both cases).

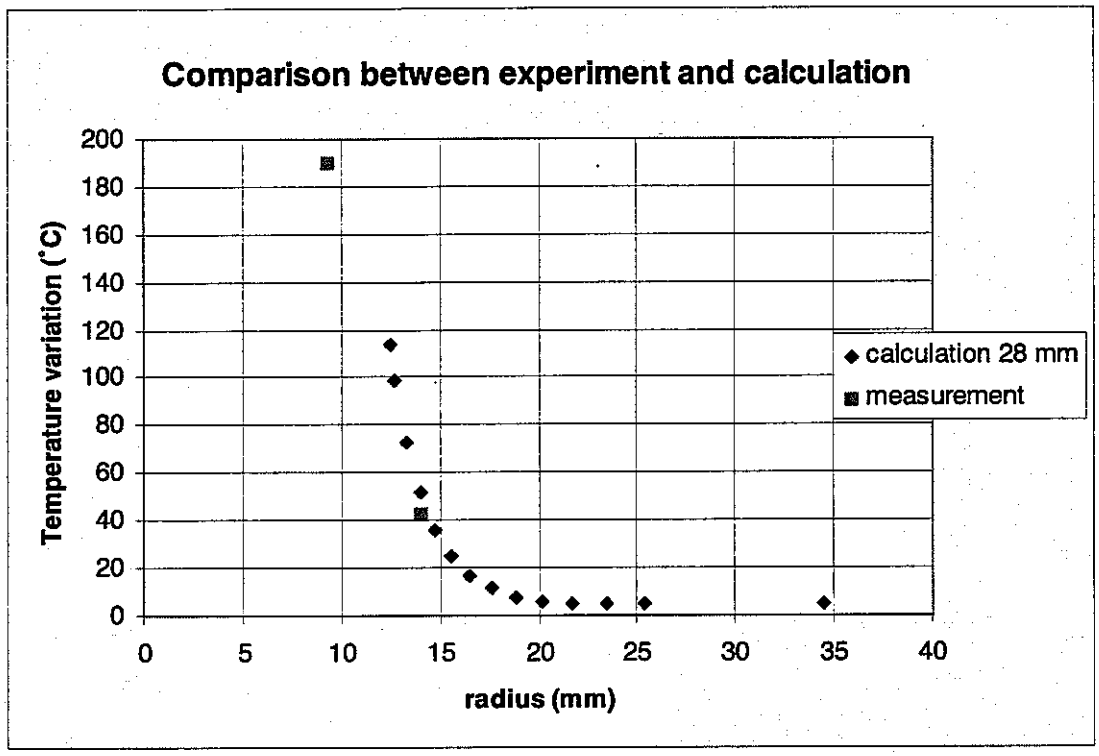

Fig.2.4 : result of calculations compared to experiment for the frequency 0.3Hz

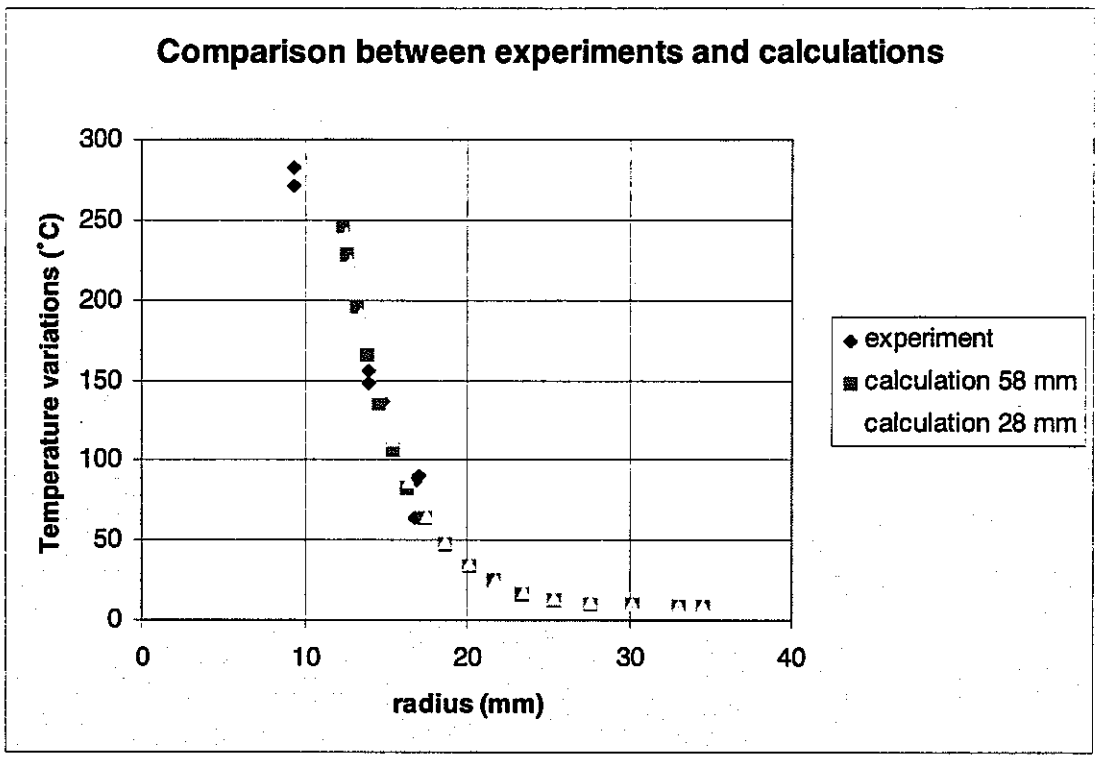

Fig.2.5 : result of calculations compared to experiment for the frequency 0.07Hz

In fact, additional calculations have been made with a one dimensionnal thermal code (Thercyl). Representing sodium flow by convection heat exchange with a coefficient of 18000 W/m2/°C (obtained by mean of Skupinski correlation), the temperature inside the tubes have been calculated. We give the comparison between the two kind of calculations in the table below :

Table 2.5 : comparison of two different thermal calculations for location z = 43 mm

	Finite Element 0.07Hz	Thercyl 0.07Hz	Finite Element 0.3Hz	Thercyl 0.3Hz
surface temperature (°C)	250	216	112	119

Surface temperature of Thercyl analyses are in good agreement with finite element fittings.

Then we have used the finite element temperature fields to estimate the stress inside FAENA tubes as explained therafter.

2.2.2. MECHANICAL ANALYSES

2.2.2.1. RESULT OF CALCULATIONS

Using the mechanical characteristics of table 2.6 (mean values of RCC-MR for 316L(N) at 370°C), the previous thermal cycles were applied with an elastic behaviour model, giving the Von Mises of Stress Variation during one cycle (figure 2.6). The displacement in z direction was fixed for one point of the specimen.

Table 2.6 : mechanical characteristics of 316L(N) at 370°C

coefficent of thermal expansion	Young Modulus	Poisson coefficient
α ($^{\circ}C^{-1}$)	E (MPa)	ν
$17.8\ 10^{-6}$	163000	0.3

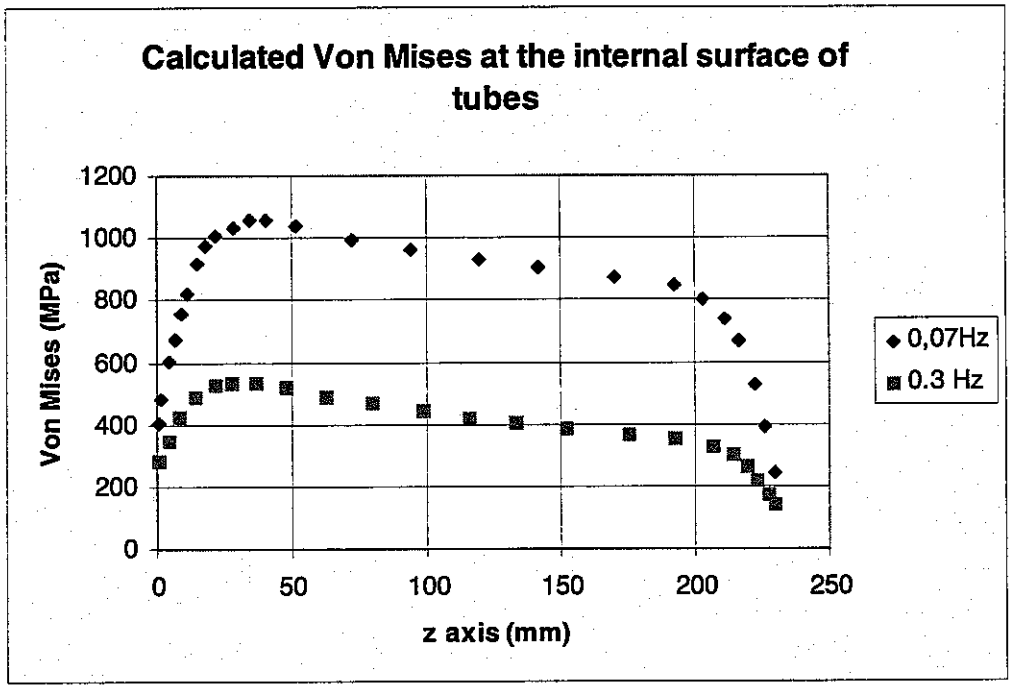

Fig 2.6: equivalent of stress variations calculated during one cycle ; comparison between 0.3 and 0.07Hz

It can be seen that at the level where the crack initiated (60 mm), the equivalent of stress variation was equal to $\Delta \sigma_{él}$ = 488 MPa for frequency 0.3Hz. At the level of maximum stress, the equivalent of stress variation reaches $\Delta \sigma_{él}$ = 1043 MPa for frequency 0.07Hz.

2.2.2.2. APPLICATION OF RCC-MR CODE

The procedure of RCC-MR design code for pure thermal fatigue is simple to apply. We shortly describe the procedure, in case of fully kinematic loading (i.e. displacement controled), by the following chart :

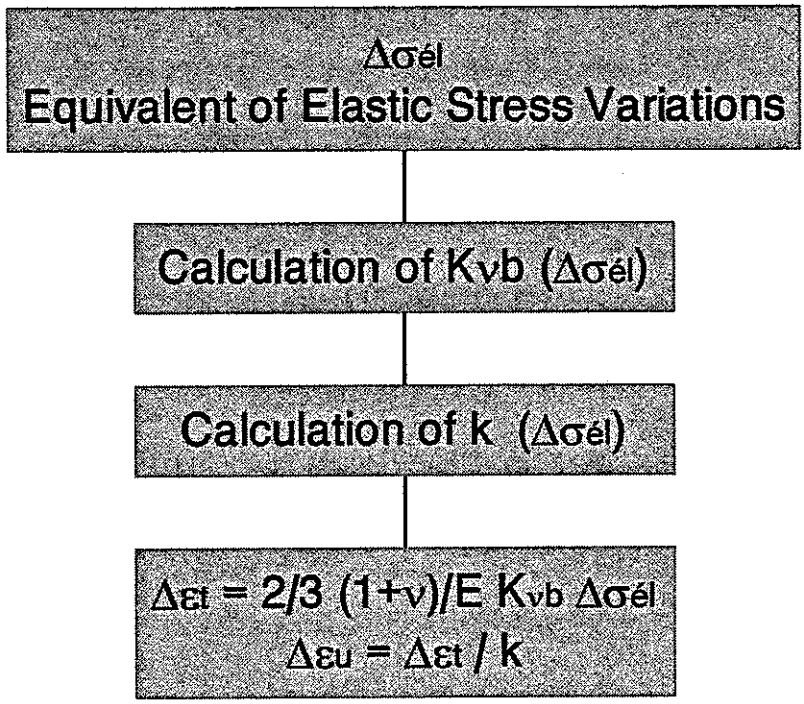

The application is easy since there is no need to account for plasticiy correction (by Neuber rule) in case of strain controlled loading. $K\nu b$ is a coefficient which represent the difference of triaxiality between elastic and elasto-plastic behaviour (it depends of the elastic stress variation, and varies between 1 for elastic cases to 1.615 for fully plastic behaviour). A particular formula in the case of biaxial stress is given by :

$$K\nu = \left(\frac{1+\bar{\nu}}{1+\nu}\right)\left(\frac{1-\nu}{1-\bar{\nu}}\right) \qquad (2.2)$$

and the general case is explained in the RCC-MR. In these equation, $\bar{\nu}$ is defined by the cyclic stress-strain curve linking the plastic strain variation $\Delta \varepsilon_p$ to the true stress variation $\Delta \sigma$:

$$\bar{\nu} = \nu\left(\frac{Es}{E}\right) + \frac{1}{2}\left(\frac{E - Es}{E}\right) \tag{2.3}$$

The secant modulus Es is simply obtained with :

$$\frac{100}{Es} = \frac{100}{E} + \frac{\Delta\varepsilon_p}{\Delta\sigma} \tag{2.4}$$

Coefficient k is not strictly speaking included in the RCC-MR ; this coefficient is required if the point has to be compared with an uniaxial fatigue curve (k coefficient permits to transform an equivalent strain variation to an uniaxial one. It's value varies from 0.8666 for pure elastic behaviour to 1 for fully plastic behaviour) :

$$k = \frac{2}{3}(1 + \bar{\nu}) \tag{2.5}$$

It is easy to calculate the equivalent strain variation profile along z axis as shown on figure 2.7 :

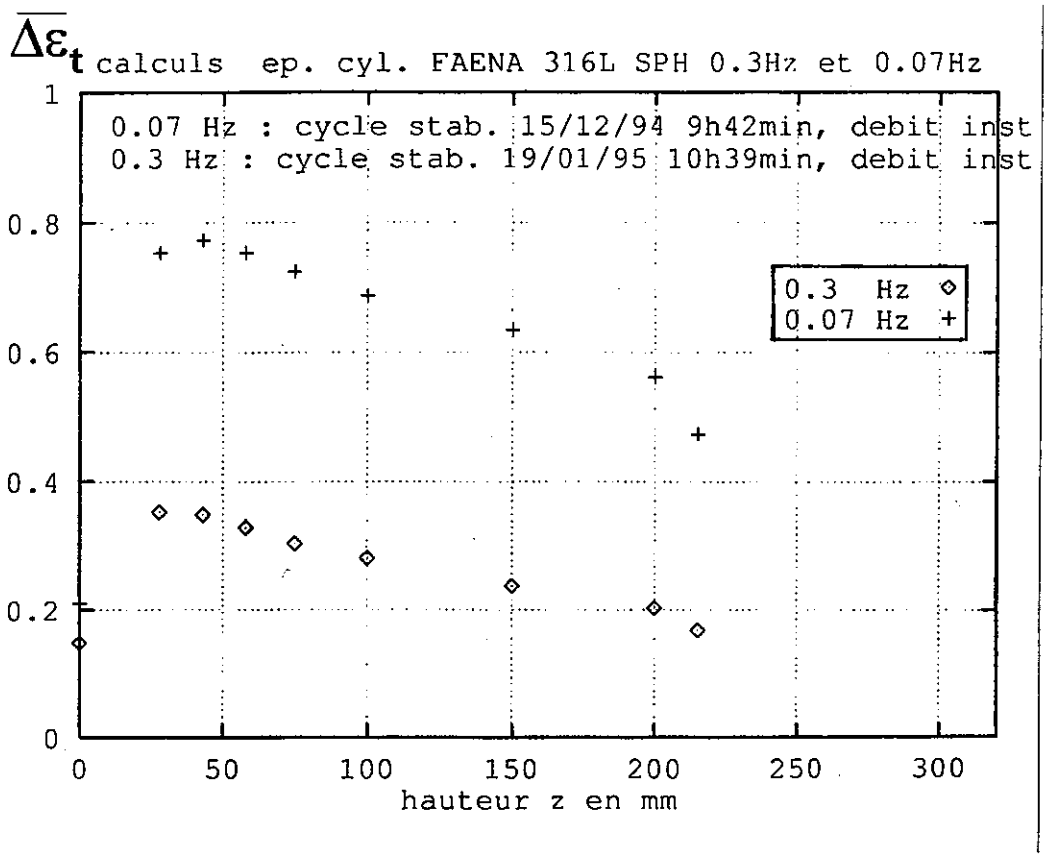

Fig 2.7: equivalent strain variation at the surface versus z axis, calculated for FAENA 3rd serie

More details on the coefficients and the calculated values are given on table 2.7 and 2.8 :

Table 2.7 : calculated strain variations for 0.07Hz test

z (mm)	$\overline{\Delta\sigma_{el}}$ (MPa)	K_{vb}	k	$\overline{\Delta\varepsilon_t}$ (%)	$\Delta\varepsilon_{tu}$ (%)
0	327.3	1.098	0.8946	0.210	0.235
28	1019.6	1.276	0.9376	0.753	0.803
43	1042.9	1.279	0.9384	0.773	0.824
58	1015	1.276	0.9376	0.753	0.803
74.97	981.2	1.270	0.9363	0.724	0.773
99.87	939.8	1.262	0.9347	0.687	0.735
149.65	872.2	1.251	0.932	0.634	0.680
199.45	786.3	1.232	0.9279	0.561	0.605
215.29	670.2	1.207	0.922	0.473	0.513

Table 2.8 : calculated strain variations for 0.3Hz test

z (mm)	$\overline{\Delta\sigma_{el}}$ (MPa)	K_{vb}	k	$\overline{\Delta\varepsilon_t}$ (%)	$\Delta\varepsilon_{tu}$ (%)
0	239.3	1.062	0.885	0.148	0.167
28	520.1	1.164	0.9117	0.352	0.386
43	515.4	1.163	0.9115	0.348	0.382
58	488.1	1.155	0.9094	0.328	0.361
74.97	459.3	1.144	0.9066	0.303	0.334
99.87	423.8	1.134	0.904	0.280	0.310
149.65	368.5	1.112	0.8984	0.2374	0.264
199.45	320	1.094	0.8935	0.203	0.227
215.29	269.9	1.074	0.888	0.168	0.189

2.2.2.3. CHOICE OF FATIGUE CURVES

The result of calculations are compared with several uniaxial fatigue curves we have to describe (see figure 2.8). It is recalled that the number of cycles to initiation correspond to the number of applied cycles in the case of FAENA tests (see paragraph 2.1 describing the principle of interpretations for more details).

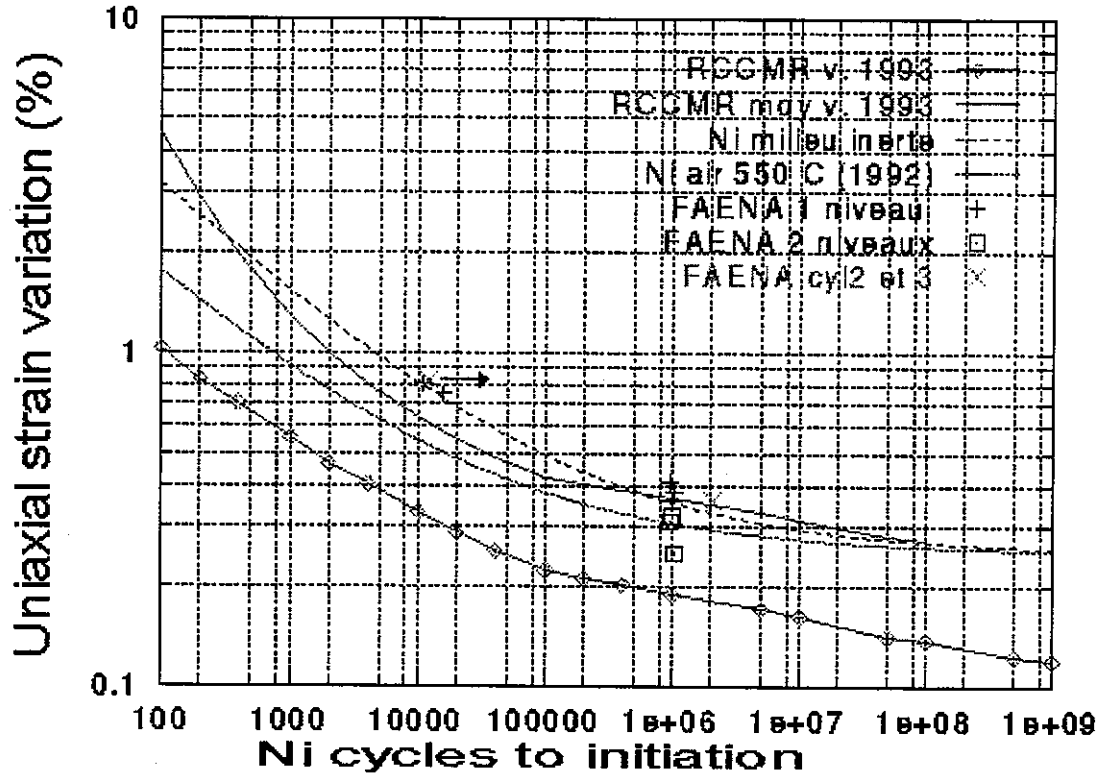

Fig. 2.8 : results of FAENA 3rd serie compared to several fatigue curves

On the figure 2.8 :

- « FAENA 1 niveau » and « FAENA 2 niveaux» are results of Y. Bargamaschi tests on FAENA sodium loop
- « FAENA cyl2 et 3 » are the present results of the 3rd serie.
- « RCC-MR v. 1993 » is the RCC-MR design curve for 316L(N) at 550°C (modified to an uniaxial curve by mean of k factor)
- « RCC-MR moy v. 1993 » is a mean fatigue deduced from the precedent by design margins reduction (a factor 2 on the strain at high cycle numbers, a facteur 20 on number of cycles for high strain levels)
- « Ni air 550°C (1992) » is an « initiation » fatigue curve builded from the Mottot fatigue results on 316L(N) at 550°C, in air environment
- « Ni milieu inerte » is an « initiation » fatigue curve builded from various sources on type 316 steels , in inert environment

This rather complicated comparison shows several particular points :

- only small differences are seen with oldest FAENA results
- inert environment has a small effect on the fatigue strength

- FAENA results are more consistent with results obtained on inert environment (except « FAENA 2 niveaux » which were tests with prior high strain fatigue damage), which conclusion seems normal as FAENA tests were performed in high purity sodium environment.

Rep essai	F (Hz)	N	dm (m^3/h)	Ra (µm)	T_m (°C)	Z (mm)	ΔT(z) (°C)	$\overline{\Delta\varepsilon}$ (z) (%)	T_{max} (°C)	$\overline{\Delta\varepsilon}$ tu (%)	Na	N/Na
Cyl2	0,3	2,098 x 10^6	0,712	0,1 - 0,3	370	60	103	0,327	422	/	9,1 x 10^5	2,305
Cyl3	0,07	1,21 x 10^4	0,727	0,1 - 0,3	370	43	256	0,773	498	/	10^4	1,21
						Pas d'amorçage						

3. JNC EVALUATION

3.1. THERMAL STRESS EVALUATION

(1) Frequency response function method

Frequency response function method [2] was utilized to evaluate thermal stress ranges on the structural surfaces induced by fluid temperature fluctuation.

JNC procedure based on the frequency response method is summarized here. The first step is identification of the following parameters from frequency of temperature fluctuation, heat transfer coefficient and material properties of structures.

Non-dimensional frequency :

$$f^* = \frac{fL^2}{a} \tag{3.1}$$

Biot number :

$$Bi = \frac{hL}{\lambda} \tag{3.2}$$

The second step is determination of the effective heat transfer function,

$$H = \mathrm{H}\left(B_i, jf^*\right) \tag{3.3}$$

from above two parameters. Both a formula and a following diagram provide gains of effective heat transfer function as a function of non-dimensional frequency and Biot number.

By using effective heat transfer function, temperature amplitude and the maximum temperature on the structural surface was determined from fluid temperature as

$$\Delta T_s = |H| \Delta T_f \tag{3.4}$$

$$T_{s\max} = T_{fm} + \frac{1}{2}|H|\Delta T_f \tag{3.5}$$

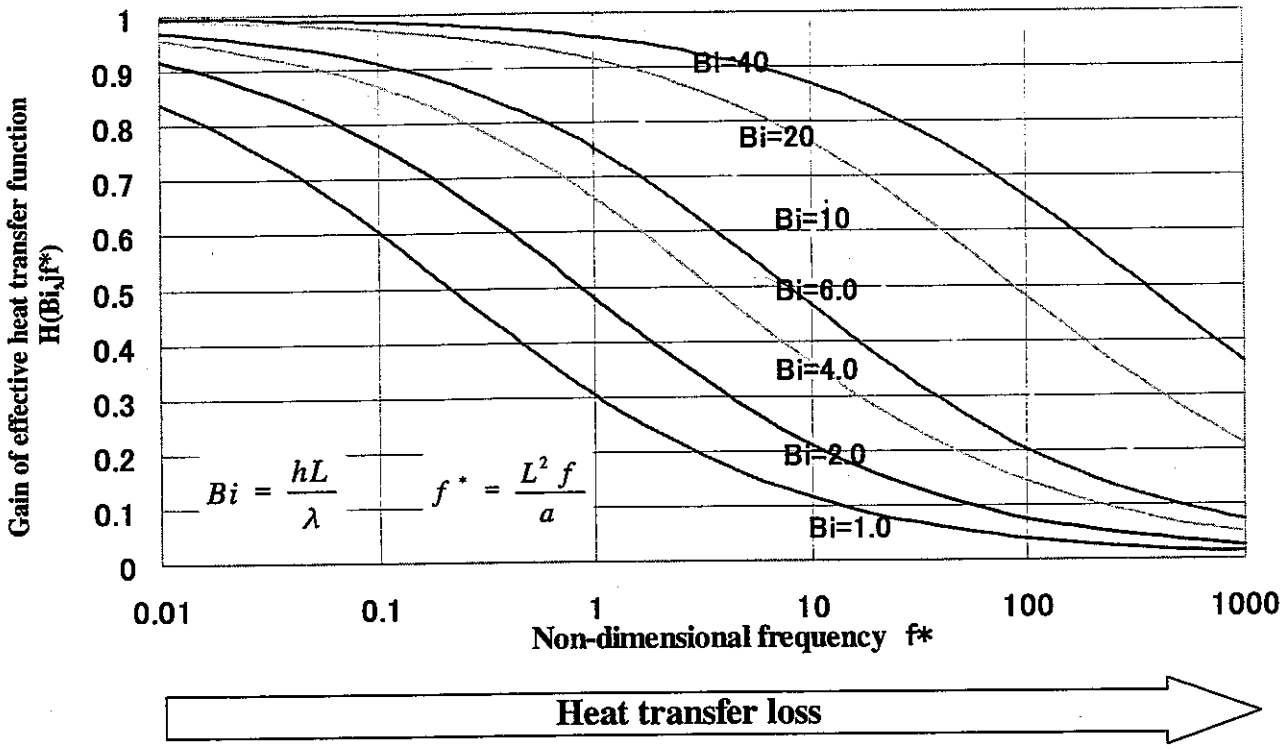

Fig.3.1 Gain of effective heat transfer function

The next step is evaluation of the effective thermal stress function

$$S = S(jf^*). \tag{3.6}$$

Since this function depends on non-dimensional frequency and constraint conditions, it is required to grasp constraint conditions of structures as (a) constraint free, (b) bending constraint and (c) membrane plus bending constraint as in Fig.3.2. Both formulae and following diagrams give gains of effective heat transfer function for each case of constraint condition.

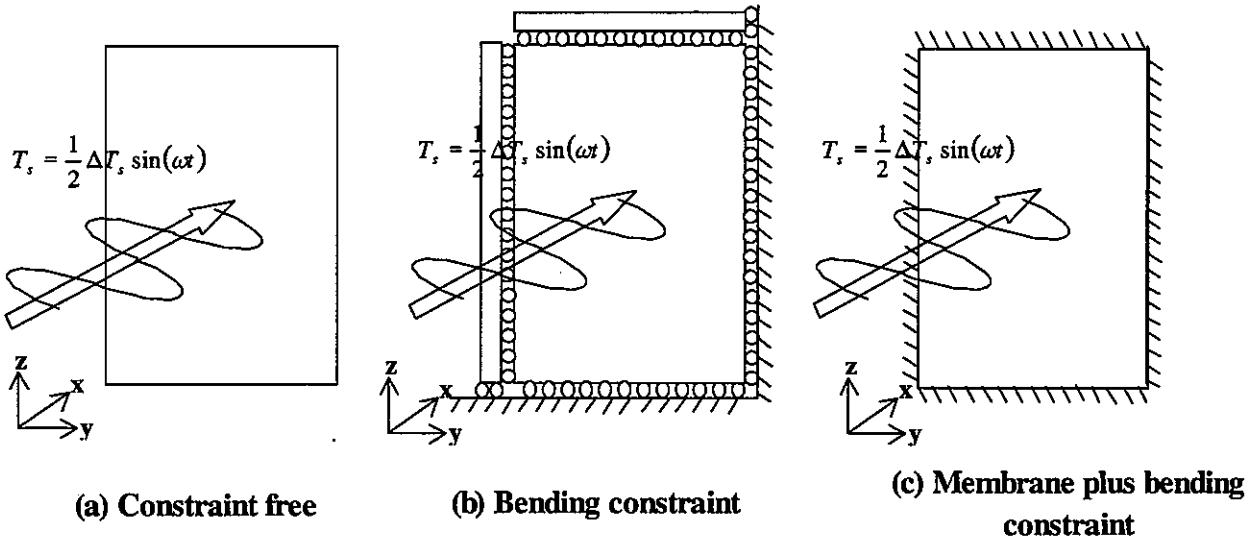

Fig. 3.2 Variations of constraint conditions

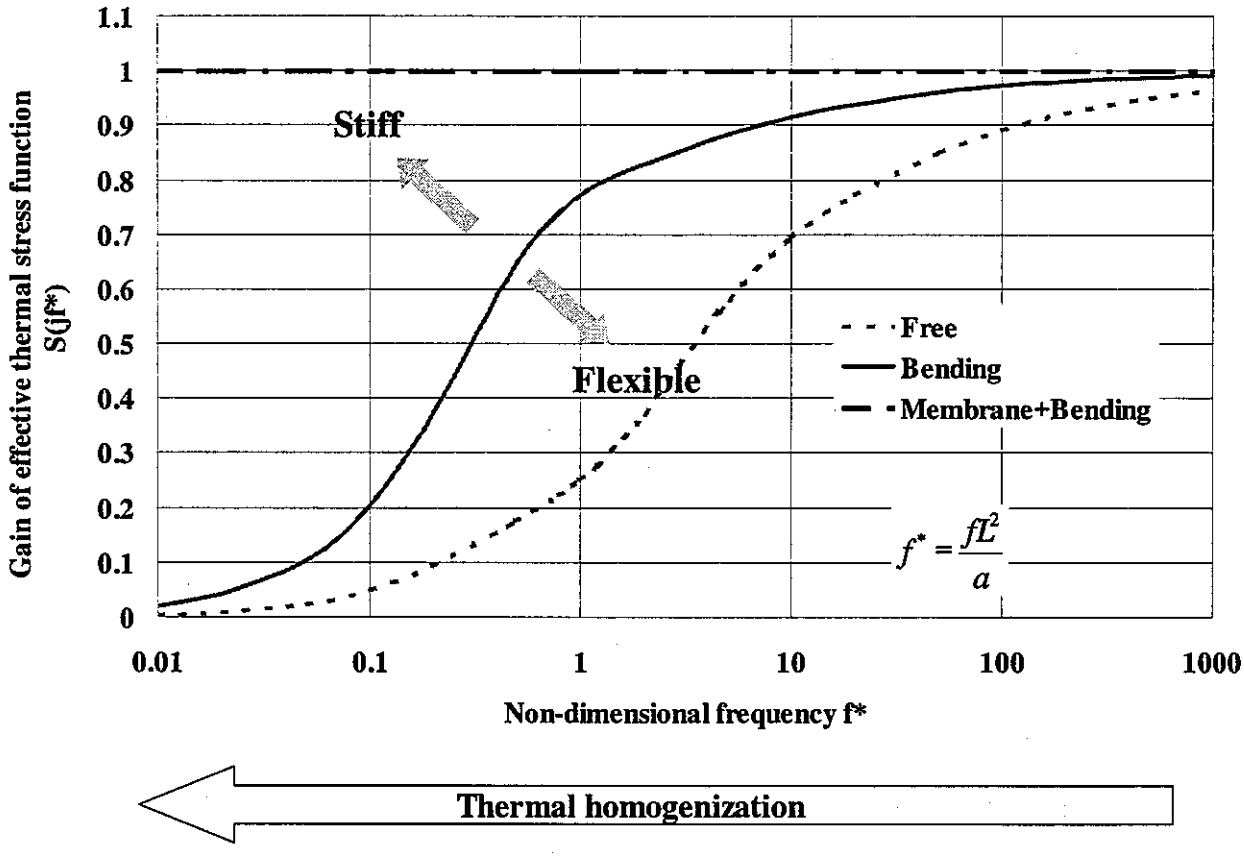

Fig.3.3 Gain of effective thermal stress function

Multiplication of $H(B_i, jf^*)$ and $S(jf^*)$ becomes the frequency response function of thermal stress to fluid temperature as

$$G(B_i, jf^*) = H(B_i, jf^*)S(jf^*). \tag{3.7}$$

Both formulae and the following diagrams provide gains of frequency response functions for three kinds of constraint conditions.

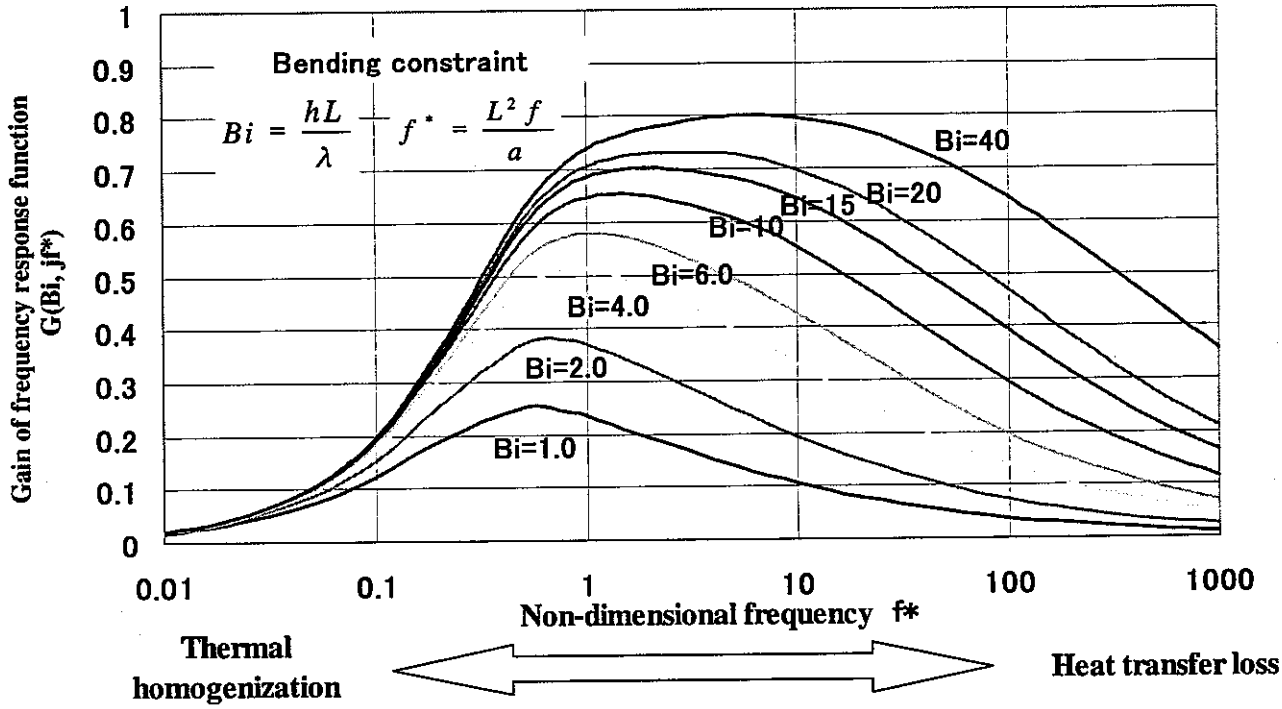

Fig.3.4 Gain of frequency response function of thermal stress to fluid temperature fluctuation (Bending constraint condition)

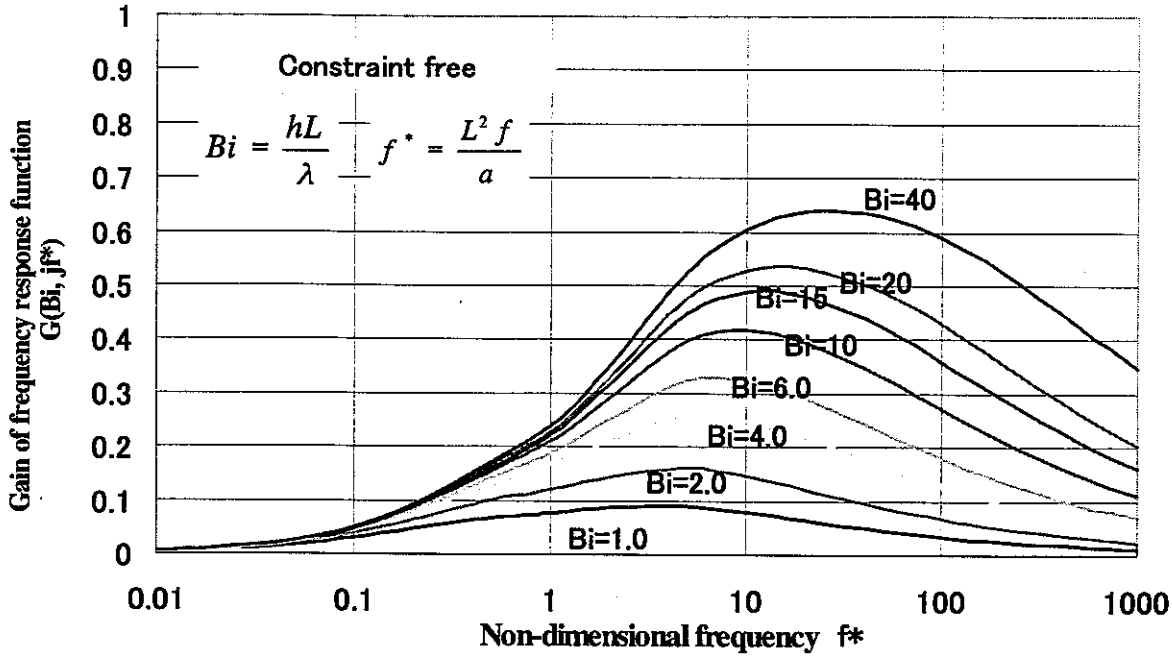

Fig.3.5 Gain of frequency response function of thermal stress to fluid temperature fluctuation (Constraint free condition)

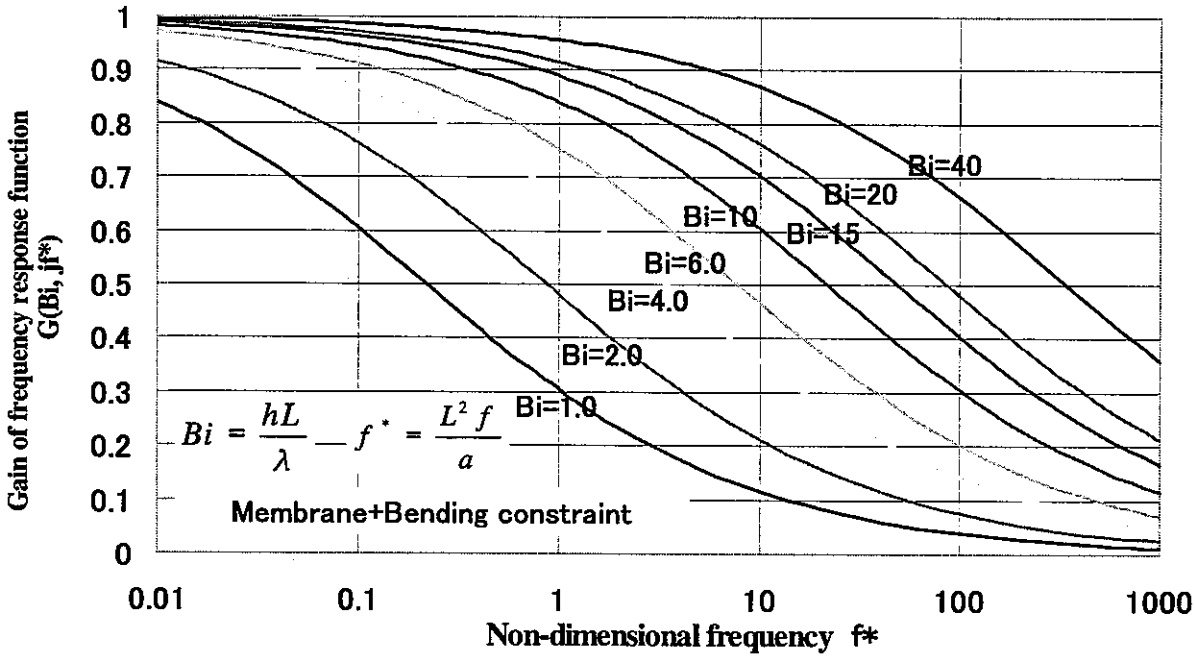

Fig.3.6 Gain of frequency response function of thermal stress to fluid temperature fluctuation (Membrane plus bending constraint condition)

The final step is evaluation of stress range on the surface. Ideal stress range converted from hundred percent of fluid temperature range is

$$\Delta\sigma_i = KE\alpha\Delta T_f \ , \tag{3.8}$$

where K is stress index determined by mechanical boundary conditions and material properties, and becomes

$$K = 1/(1-\nu) \tag{3.9}$$

in the case of biaxial plane stress condition.

By using gain of the frequency response function, actual stress range on the surface can be evaluated from ideal stress range as

$$\Delta\sigma\big|_{x=0} = \Delta\sigma_i \left| G\left(B_i, jf^*\right) \right| . \tag{3.10}$$

(2) Evaluation of FAENA 3rd

Average of fluid temperature of the FAENA 3rd experiment is 370 ℃. By using material properties of 316L(N) at 370℃ [4] and wall thickness 22.05mm, non-dimensional frequencies were calculated from actual ones.

Heat transfer coefficient 18000 W/m^2/h/℃ [2] was also translated to Biot number.

Results are described in the next table.

Table 3.1 Non-dimensional parameters of FAENA 3rd

Frequency f (Hz)	Non-dimensional frequency f*	Biot number Bi
0.07	7.65	20.9
0.3	32.8	

From above two parameters, gains of the effective heat transfer function were determined as in the next figure.

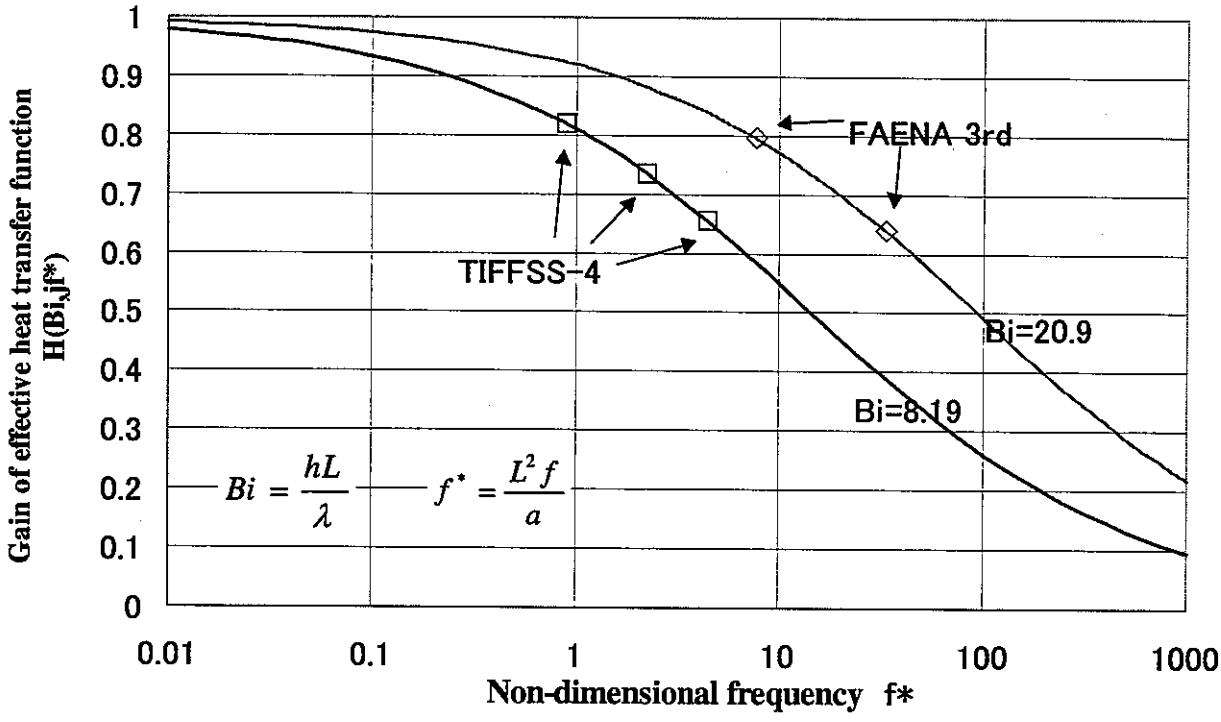

Fig.3.7 Gain of effective heat transfer function of FAENA 3rd and TIFFSS-4

The effective heat transfer function evaluated temperature amplitude and the maximum temperature on the structural surface from fluid temperature as in the next table.

Table 3.2 Temperature on the surface of FAENA 3rd specimen

Frequency (Hz)	Gain of effective heat transfer function	Fluid temperature range (deg)	Temperature range on the surface(deg)	Maximum temperature on the surface(deg)
0.07(Inlet)	0.796	289	230	485
0.07(z=43mm)	0.796	268	213	477
0.07(Outlet)	0.796	202	161	450
0.3(Inlet)	0.640	200	128	434
0.3(z=60mm)	0.640	158	101	421
0.3(Outlet)	0.640	100	64	402

Since specimens of FAENA 3rd are thick cylinders, they have a bending constraint condition. The effective thermal stress function under a bending constraint condition was determined as a function of non-dimensional frequency. Gains of this function are shown in the next figure.

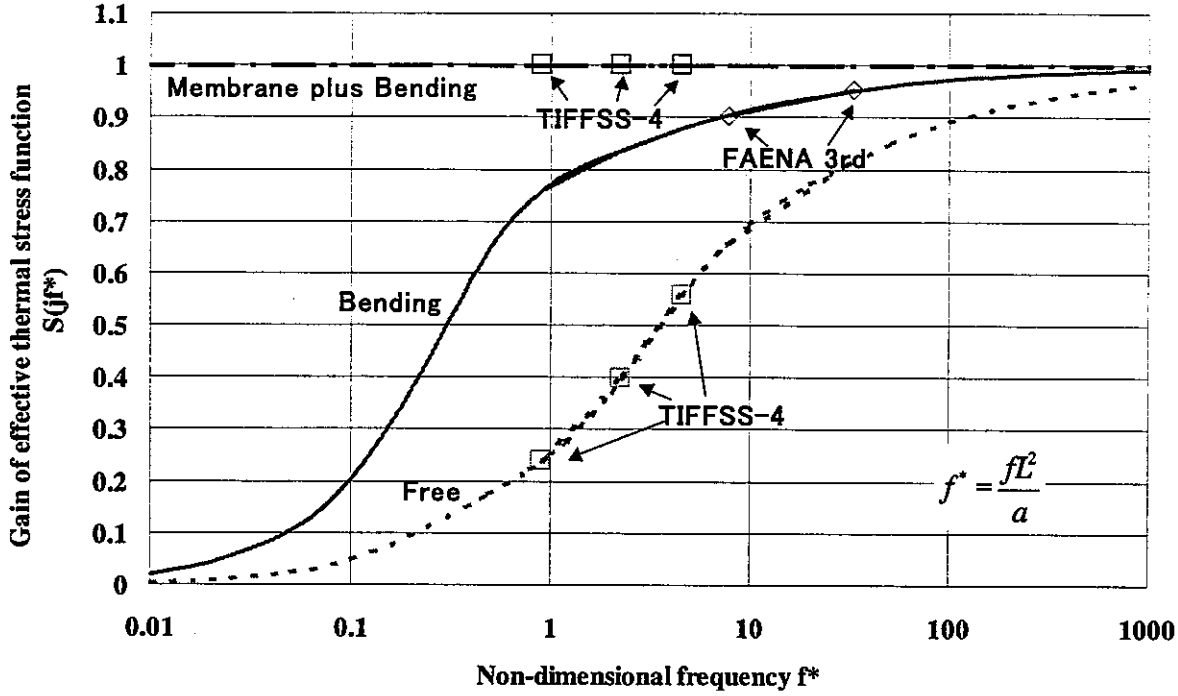

Fig.3.8 Gain of effective thermal stress function of FAENA 3rd and TIFFSS-4

By multiplying $H(B_i, jf^*)$ and $S(jf^*)$, frequency response function of thermal stress was determined and its gain is shown in the next diagram.

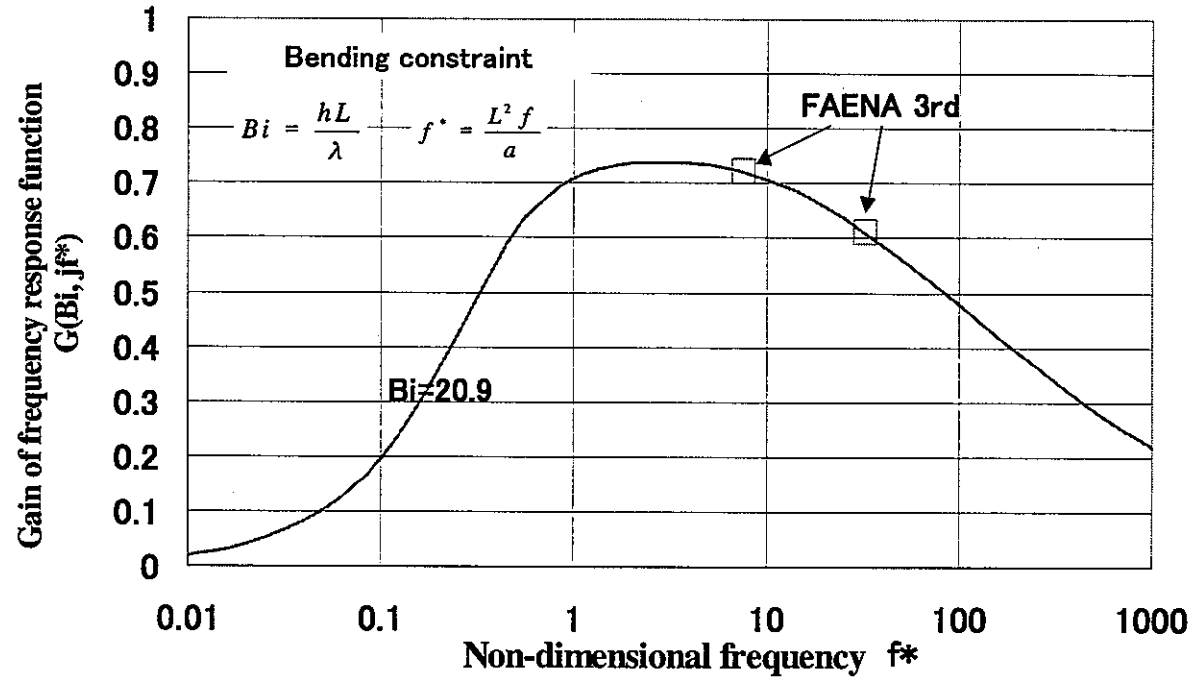

Fig.3.9 Gain of frequency stress response of FAENA 3rd

The frequency response function calculated actual stress ranges on the surface from ideal stress ranges, which were obtained from fluid temeperature range with material properties of 316L(N).

Results are as in the next table.

Table 3.3 Stress range of FAENA 3rd

Frequency (Hz)	Gain of effective thermal stress function	Gain of frequency response function	Ideal stress range (MPa)	Stress range on the surface (MPa)
0.07(Inlet)	0.904	0.719	1290	927
0.07(z=43mm)	0.904	0.719	1195	859
0.07(Outlet)	0.904	0.719	901	648
0.3(Inlet)	0.952	0.609	892	544
0.3(z=60mm)	0.952	0.609	706	430
0.3(Outlet)	0.952	0.609	446	272

(3) Evaluation of Tiffss-4

Average of fluid temperature of the Tiffss-4 experiment is 350 ℃. By using material properties of 316FR at 350℃ and wall thickness 10mm, non-dimensional frequencies were calculated from actual ones.

Heat transfer coefficient 13300 kcal/m^2/h/℃ [2] was also translated to Biot number. Results are described in the next table.

Table 3.4 Non-dimensional parameters of TIFFSS-4

Frequency f (Hz)	Non-dimensional frequency f*	Biot number Bi
0.04	0.906	8.16
0.1	2.26	
0.2	4.53	

Above two parameters determined the effective heat transfer function, gain of which is shown in Fig.3.7.

The heat transfer function evaluated temperature amplitudes and the maximum temperature on the structural surface from fluid temperature as in the next table

Table 3.5 Temperature on the surface TIFFSS-4 specimen

Frequency (Hz)	Gain of effective heat transfer function	Fluid temperature range (deg)	Temperature range on the surface(deg)	Maximum temperature on the surface(deg)
0.04	0.817	240	196	448
0.1	0.733	240	176	438
0.2	0.653	240	157	428

The plane plate specimen of TIFFSS-4 has a constraint free condition and the other specimen with thermal insulator is considered as bending plus membrane constraint conditions. So that, effective thermal stress functions were determined for both conditions. Gains of these functions are shown in Fig.3.8.

The frequency response functions obtained by multiplying $H(B_i, jf^*)$ and $S(jf^*)$ have gains as in the next diagrams.

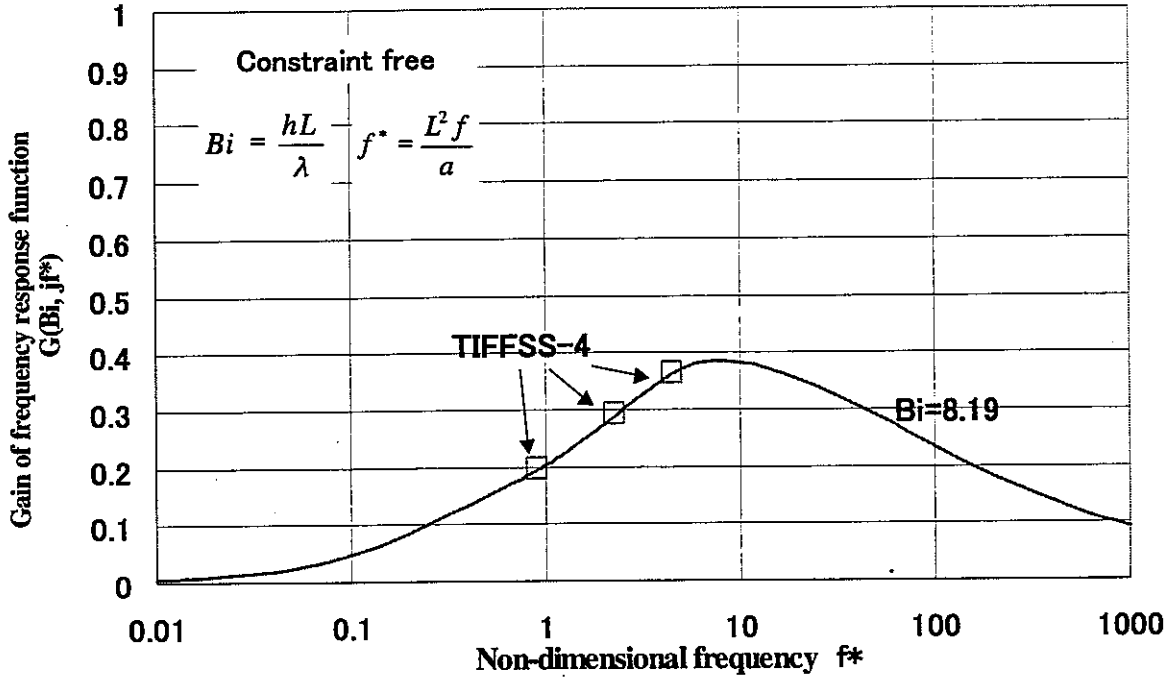

Fig.3.10 Gain of frequency stress response of TFFSS-4 (Constraint free)

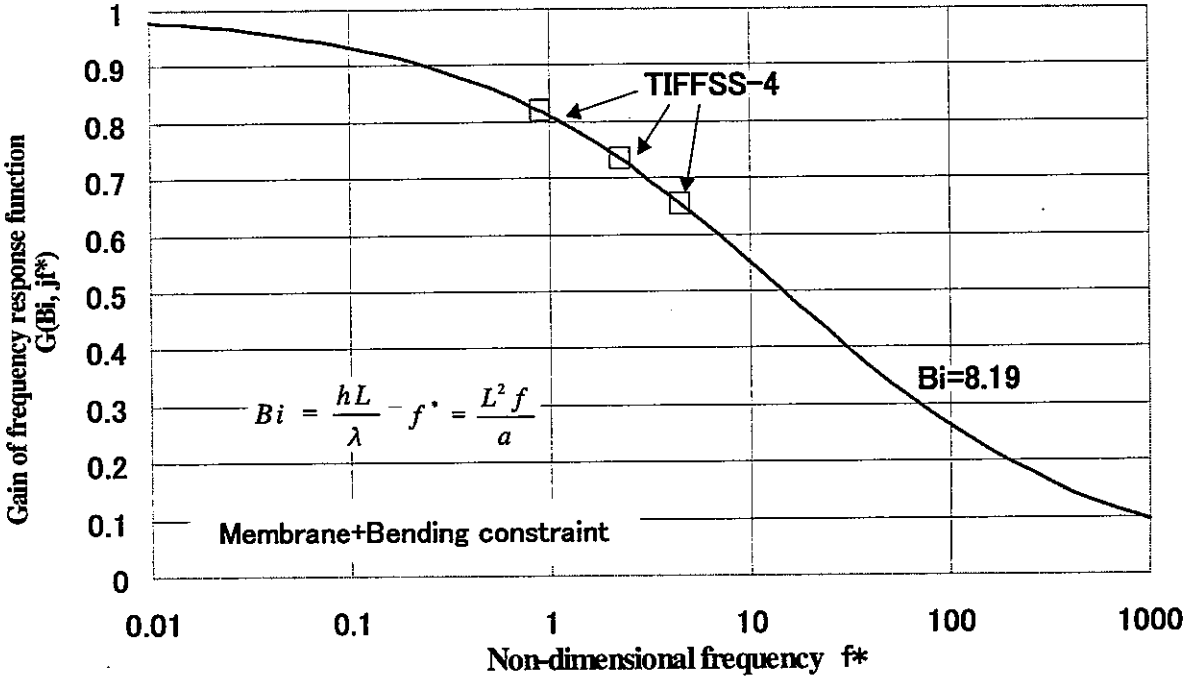

Fig.3.11 Gain of frequency stress response of TFFSS-4
(Membrane plus bending constraint)

The frequency response functions evaluated actual stress ranges on the surface under both constraint conditions from ideal stress ranges, which were obtained from fluid temperature range with material properties of 316FR. Results are as in the next tables.

Table 3.6 Stress range of TIFFSS-4 (Constraint free)

Frequency (Hz)	Gain of effective thermal stress function	Gain of frequency response function	Ideal stress range (MPa)	Stress range on the surface (MPa)
0.04	0.239	0.195	1120	218
0.1	0.399	0.292	1120	327
0.2	0.558	0.365	1120	409

Table 3.7 Stress range of TIFFSS-4 (Membrane plus bending constraint)

Frequency (Hz)	Gain of effective thermal stress function	Gain of frequency response function	Ideal stress range (MPa)	Stress range on the surface (MPa)
0.04	1.000	0.817	1120	915
0.1	1.000	0.733	1120	821
0.2	1.000	0.653	1120	732

3.2. STRAIN CONCENTRATION AND FATIGUE EVALUATION

(1) Evaluation procedure

Considering strain enhancement from plasticity, JNC procedure estimates total strain range $\overline{\Delta\varepsilon_{tot}}$ from elastically calculated equivalent stress range $\overline{\Delta\sigma}$ [8].

In this procedure, general equation for considering both local strain concentration and global strain redistribution is expressed as

$$\overline{\Delta\varepsilon_{tot}} = KKe'_L Ke'_G \overline{\Delta\varepsilon_n} . \tag{3.11}$$

$$\overline{\Delta\varepsilon_n} = \frac{S_n}{E} , \tag{3.12}$$

where S_n is stress intensity range. Since thermal stress induced by thermal striping is local bending and peak stress, Eq.(3.11) can be reduced to

$$\overline{\Delta\varepsilon_{tot}} = Ke'\overline{\Delta\varepsilon_e} \tag{3.13}$$

$$\overline{\Delta\varepsilon_e} = \frac{\overline{\Delta\sigma}}{E} \tag{3.14}$$

$$Ke' = \{1 + (q - 1)(1 - \frac{2\sigma_y}{\Delta\sigma})\} , \tag{3.15}$$

where q is an elastic follow-up parameter and can be adjusted to $q = 5/3$, when stress is generated by temperature gradient across wall thickness[9] .

The evaluated strain range $\overline{\Delta\varepsilon_{tot}}$ predicts an allowable cycle number $N_f\left(\overline{\Delta\varepsilon_{tot}}\right)$ from fatigue curves of material at the maximum temperature. Here, JNC procedure takes strain rate effect into account. *Miner's* rule evaluates fatigue damage factor Df as

$$D_f = \sum \frac{N\left(\overline{\Delta\varepsilon_{tot}}\right)}{N_f\left(\overline{\Delta\varepsilon_{tot}}\right)} \tag{3.16}$$

where, $N\left(\overline{\Delta\varepsilon_{tot}}\right)$ is the applied cycle number of strain range $\overline{\Delta\varepsilon_{tot}}$.

(2) Evaluation of FAENA 3rd

Eq.(3.13) has evaluated strain ranges on the surfaces from stress ranges. The next table shows the results.

Table 3.8 Fatigue strength evaluation of FAENA 3rd

Frequency (Hz)	Stress range on the surface (MPa)	Strain range (%)	Mamimum temperature on the surface (deg)	Allowable cycle number
0.07(Inlet)	927	0.845	485	2.96×10^3
0.07(z=43mm)	859	0.773	477	3.90×10^3
0.07(Outlet)	648	0.559	450	1.69×10^4
0.3(Inlet)	544	0.453	434	8.05×10^4
0.3(z=60mm)	430	0.337	421	2.62×10^6
0.3(Outlet)	272	0.177	402	4.04×10^{13}

The CEA benchmark problem [5] provided average fatigue data of 316L(N) for 550deg. Allowable cycle numbers were calculated by interpolation of fatigue data with the next equation as in the Table 3.8.

$$\log_{10}(N_f)^{\frac{1}{2}} = -1.6408 + 1.1781(\log_{10}\Delta\varepsilon_t) - 1.2473(\log_{10}\Delta\varepsilon_t)^2 + 4.6416(\log_{10}\Delta\varepsilon_t)^3 - 4.9241(\log_{10}\Delta\varepsilon_t)^4 \quad (3.17)$$

Eq.(3.17) can approximate fatigue data of 316L(N) adequately as in the next figure. The same figure also shows allowable cycle numbers.

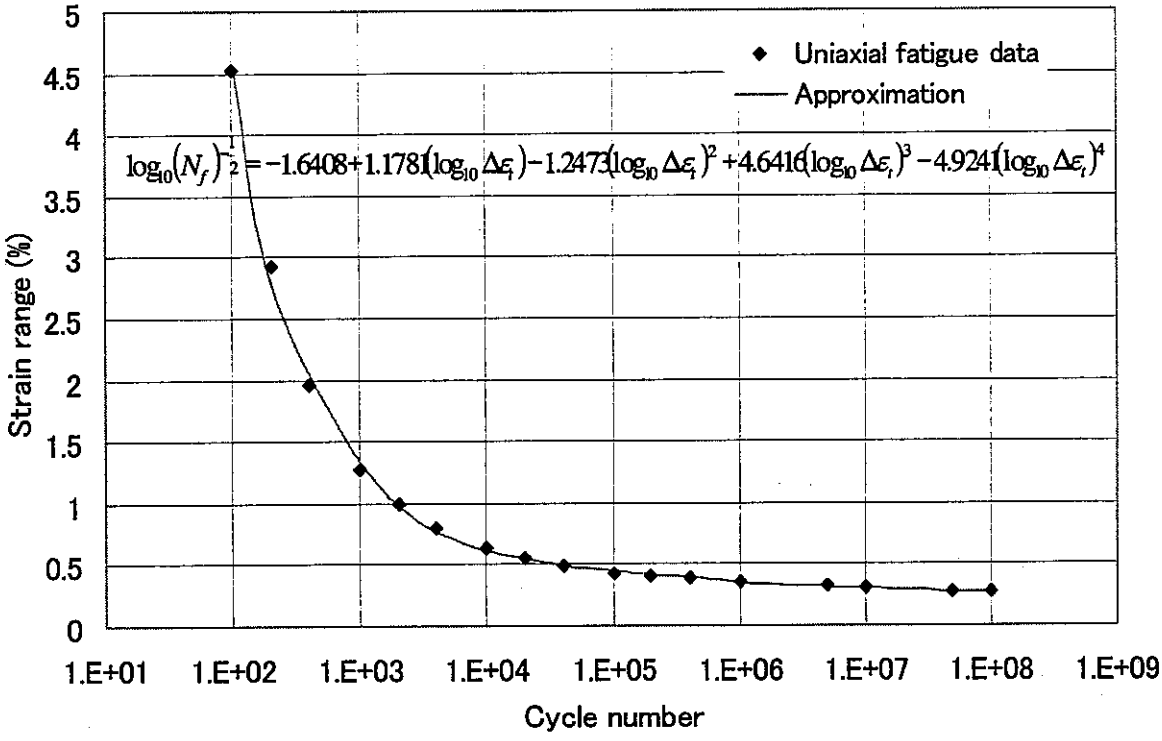

Fig. 3.12 Fatigue curve of 316L(N) with FAENA 3rd fatigue strength

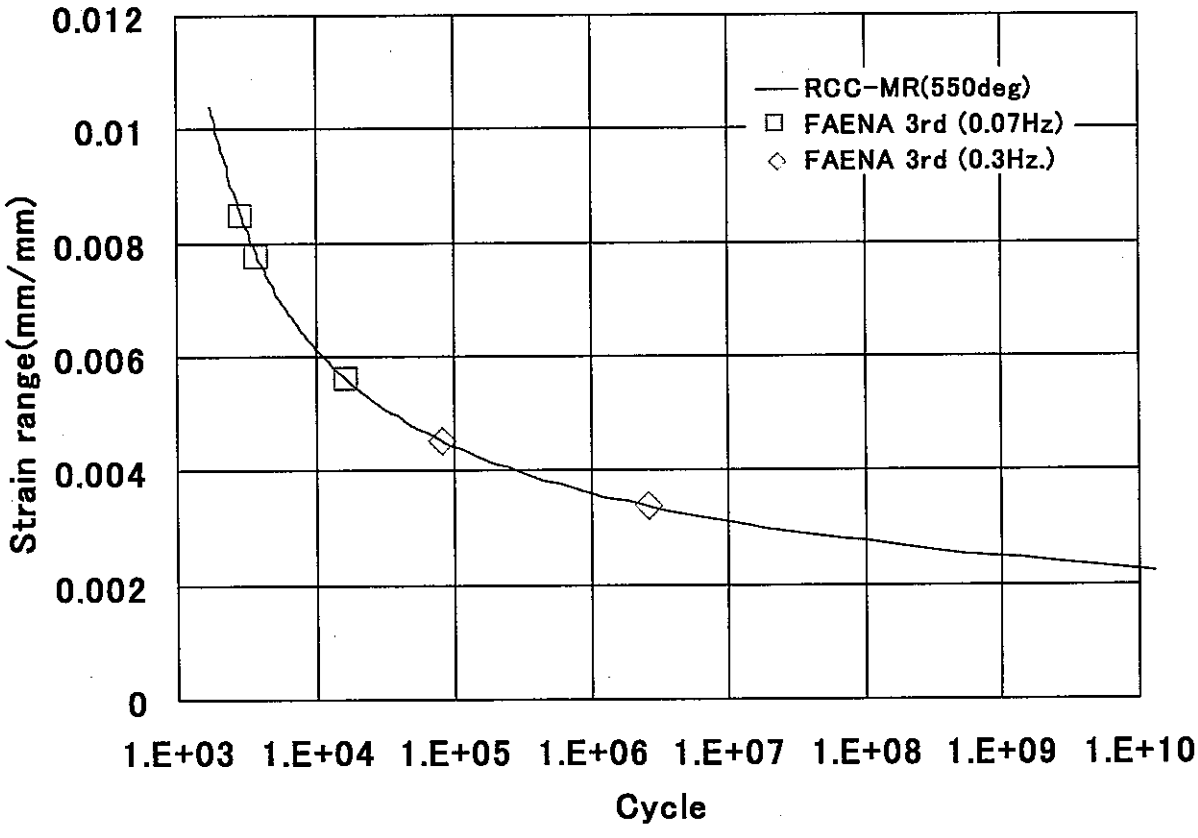

Fig. 3.13 Fatigue curve of 316L(N) with FAENA 3rd fatigue strength

Fatigue damage factors for FAENA 3rd experiment were evaluated by Eq.(3.16), results of which are shown in the next table.

Table 3.9 Fatigue damage of FAENA 3rd

Frequency (Hz)	Experimental cycle number N	Allowable cycle number Nf	N/Nf
0.07(Inlet)	1.21×10^4	2.96×10^3	4.09
0.07(z=43mm)	1.21×10^4	3.90×10^3	3.10
0.07(Outlet)	1.21×10^4	1.69×10^4	0.716
0.3(Inlet)	2.10×10^6	8.05×10^4	26.1
0.3(z=60mm)	2.10×10^6	2.62×10^6	0.801
0.3(Outlet)	2.10×10^6	4.04×10^{13}	0.000

Experimentally, the locations of crack initiation are Z=43mm at 0.07Hz and Z=60mm at 0.3Hz. Results in the Table 3.8 indicate JNC evaluation is conservative for 0.07Hz and is adequate for 0.3Hz.

(2) Evaluation of TIFFSS-4

Eq.(3.12) evaluates strain ranges on the surfaces from stress ranges. The results were described in the next table with the maximum temperature on the surface evaluated from temperature analysis.

Table 3.10 Fatigue strength evaluation of TIFFSS-4
(Constraint free)

Frequency (Hz)	Stress range on the surface (Mpa)	Strain range (%)	Mamimum temperature on the surface (deg)	Allowable cycle number
0.04	218	0.115	448	1.87×10^{15}
0.1	327	0.220	438	1.48×10^{7}
0.2	409	0.299	428	7.34×10^{5}

Table 3.11 Fatigue strength evaluation of TIFFSS-4
(Membrane plus bending constraint)

Frequency (Hz)	Stress range on the surface (Mpa)	Strain range (%)	Mamimum temperature on the surface (deg)	Allowable cycle number
0.04	915	0.788	448	5.13×10^{3}
0.1	821	0.697	438	8.67×10^{3}
0.2	732	0.611	428	1.54×10^{4}

The JNC benchmark problem provided average fatigue curves of 316FR for each temperature[1]. Allowable cycle numbers were calculated based on these curves as in the Table 3.11.

Fatigue curves of 316FR and evaluated allowable cycle numbers were plotted in the next figure.

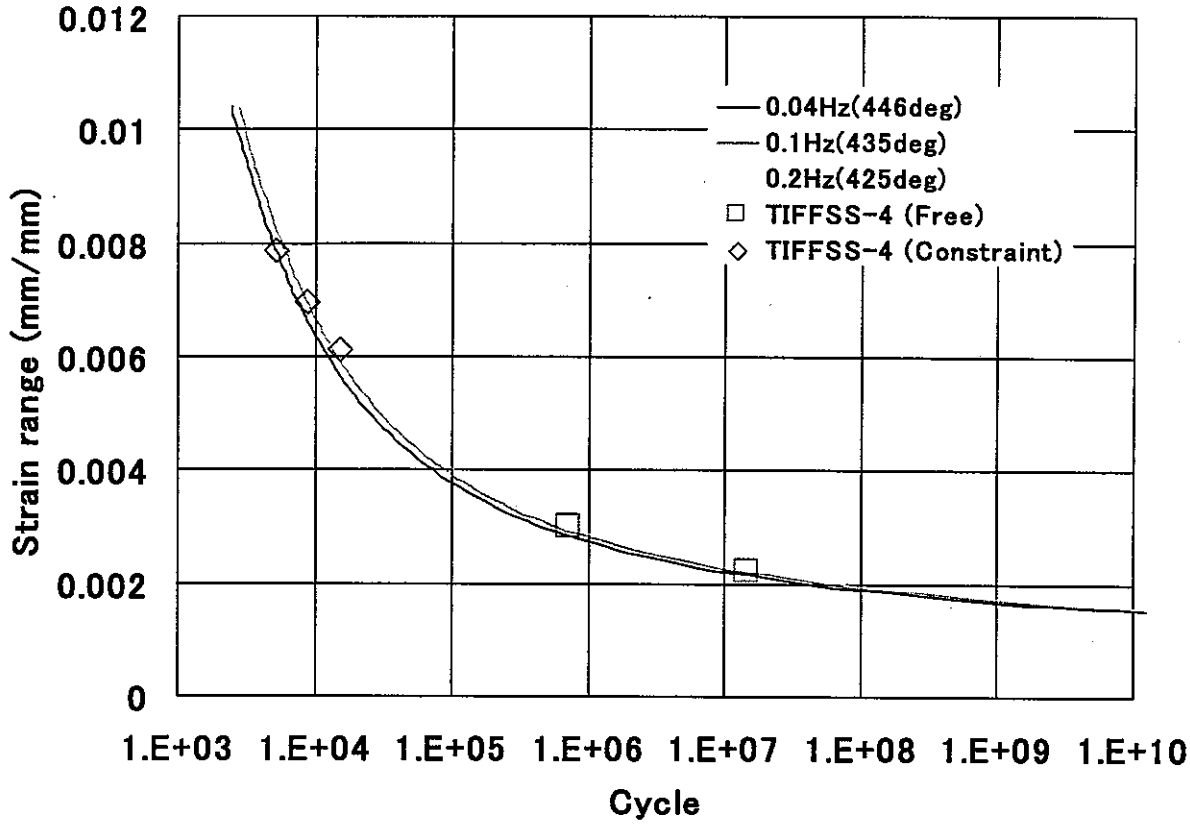

Fig. 3.14 Fatigue curve of 316FR with TIFFSS-4 fatigue strength

Eq.(3.16) evaluated fatigue damage factors for TIFFSS-4 experiment, which are shown in the next table. Results of the membrane plus bending constraint tests will be provided in near future.

Table 3.12 Fatigue damage of TIFFSS-4 (Constraint free)

Frequency (Hz)	Experimental cycle number N	Allowable cycle number Nf	N/Nf	Remarks
0.04		1.87×10^{15}		No experimental data
0.1	9×10^{4}	1.48×10^{7}	0.01	No cracks
0.2		7.34×10^{5}		No experimental data

Table 3.13 Fatigue damage of TIFFSS-4 (Membrane plus bending constraint)

Frequency (Hz)	Experimental cycle number N	Allowable cycle number Nf	N/Nf	Remarks
0.04	5×10^{3}	5.13×10^{3}	0.97	Data available in near future
0.1	1×10^{4}	8.67×10^{3}	1.15	Data available in near future
0.2	2×10^{4}	1.54×10^{4}	1.30	Data available in near future

4. INTERCOMPARISON

4.1. EVALUATION METHODS

- CEA uses finite element method to calculate stress history from temperature time history considering detailed temperature signals, for the benchmark. On the other hand, JNC evaluates stress range by the frequency response diagram with assumption of sinusoidal fluctuation.

(2) Fatigue strength evaluation method

- CEA evaluates strain range from elastically calculated stress range with two concentration factors $K\nu b$ and k for considering plasticity and multiaxiality in order to compare the results with several uniaxial fatigue curves. JNC adopted one strain concentration factor with elastic follow-up parameter for considering plasticity and multiaxiality.

4.2. EVALUATION RESULTS

(1) Stress evaluation result

- CEA evaluated slightly larger stress range than JNC. Because experimental signal is rather rectangular than sinusoidal and the former signal generates larger stress range than the later one.

(2) Fatigue strength evaluation result

- Even though strain concentration models are different, CEA and JNC evaluated similar strain concentration factors for plasticity and multiaxiality. As a result, CEA evaluated larger stress range than JNC since stress ranges are different. Finally, CEA evaluated slightly larger fatigue damages than JNC.

- A comparison with several fatigue curves showed that FAENA results are in better agreement with curves of fatigue tests performed in inert environment (curves modified to give crack initiation cycle numbers).

ACKNOWLEDGEMENT

It is very thankful in coordination of cooperative between CEA and JNC by Dr. J.C. Astegiano, Dr. C.Poette and Dr. M.T. Cabrillat of CEA-Cadarache and Dr.M.Morishita of OEC/JNC.

REFERENCES

[1] Kasahara,N. and Lejeail, Y., Benchmark problems on thermal striping evaluation of FAENA and TIFFSS sodium experiments, JNC TN9400 2001-006,(2000)

[2] Kasahara,N. , Frequency response function method for evaluation of thermal striping phenomena , JNC TN9400 2001-005,(2000)

[3] Lejeail,Y. and Kasahara,N. , Interpretation of FAENA and TIFFFSS experiments : Comparison of temperature evaluation methods on thermal striping , JNC TN9400 2001-014,(2000)

[4] RCC-MR, Design and Construction rules for mechanical components of FBR nuclear islands, AFCEN, (1993)

[5] Kasahara, N. et al., 'Advanced Creep-fatigue Evaluation Rule for Fast Breeder Reactor Components : Generalization of Elastic Follow-up Model', NED 155, pp499/518, (1995)

[6] Kasahara,N. et al.,'Strain Concentration Evaluation of Smooth Structures Subjected to Thermal Stress', JSME, Proc.of Annual Meeting of JSME/MMD,315 In Japanese,(1993)